NASA TECHNICAL NOTE

NASA TN D-2537

c. 1

LOAN COPY: RETU
AFWL (WLIL
KIRTLAND AFB, N

TECH LIBRARY KAFB, NM

0154776

NASA TN D-2537

THE EFFECT OF END SLOPE ON THE BUCKLING STRESS OF CYLINDRICAL SHELLS

by C. D. Babcock and E. E. Sechler

Prepared under Grant No. NsG-18-59 *by*
CALIFORNIA INSTITUTE OF TECHNOLOGY
Pasadena, Calif.
for

NATIONAL AERONAUTICS AND SPACE ADMINISTRATION • WASHINGTON, D. C. • DECEMBER 1964

TECH LIBRARY KAFB, NM
0154776

THE EFFECT OF END SLOPE ON THE BUCKLING STRESS OF CYLINDRICAL SHELLS

By C. D. Babcock and E. E. Sechler

Distribution of this report is provided in the interest of information exchange. Responsibility for the contents resides in the author or organization that prepared it.

Prepared under Grant No. NsG-18-59 by
CALIFORNIA INSTITUTE OF TECHNOLOGY
Pasadena, California

for

NATIONAL AERONAUTICS AND SPACE ADMINISTRATION

For sale by the Office of Technical Services, Department of Commerce,
Washington, D.C. 20230 -- Price $1.00

THE EFFECT OF END SLOPE ON THE BUCKLING STRESS OF CYLINDRICAL SHELLS

By C. D. Babcock and E. E. Sechler

California Institute of Technology

SUMMARY

Seamless cylindrical shells with $R/t \simeq 800$ were loaded with a uniform axial load to failure. The radial displacement of the boundary was controlled and the boundary slope was measured. With these values known, the maximum slope of the shell near the boundary could be calculated. If the maximum slope is plotted against the degradation of buckling stress from the classical value a definite correlation appears.

INTRODUCTION

Recent papers on the buckling of shells have focused attention on aspects of the buckling problem that have hitherto been either overlooked or ignored. Two common assumptions made in shell analyses are: 1) that one can use the membrane solution to give the state of the shell just prior to buckling and 2) that the solution is probably insensitive to the details of the boundary conditions. These concepts have been shown to be invalid by Stein (Ref. 1), Fisher (Ref. 2), Sobel (Ref. 3) and others. In fact, the effect of these "negligible" factors may be so great as to override nearly all other factors. Since the effect is so large, it should be detectable by experimental methods.

LIST OF SYMBOLS

E	Young's modulus - psi
ℓ	height of the end ring - inches
p	pressure used to displace end rings - psi
P	axial load on the shell - lb
$P_{C\ell}$	classical buckling load $= 2\pi Rt\sigma_{C\ell}$ - lb

R	shell radius - inches
t	shell thickness - inches
α_o	boundary slope of the shell - radians
$\alpha(x)$	slope of the shell at any distance x from the boundary - radians
δ_o	boundary displacement of the shell - inches
δ_R	displacement of the end rings - inches
δ_S	radial displacement of the central portion of the shell - inches
δ^*	shell displacement due to end ring rotation - inches
ν	Poisson's ratio
σ_{axial}	axial stress - psi
$\sigma_{C\ell}$	classical buckling stress $= \frac{E}{\sqrt{3(1-\nu^2)}} \frac{t}{R}$ - psi
σ_p	proportional limit stress - psi

EXPERIMENTAL PROGRAM

In an effort to verify experimentally that slight changes at the shell boundary might lead to major changes in the buckling stress, a cylindrical shell was subjected to an axial buckling load while, at the same time, the shell boundaries were given a controlled radial displacement. In the usual experiment, the ends of the shell are attached in some manner to end rings and the shell is loaded through these rings. As the axial load is increased, the shell wall trys to expand radially due to the Poisson ratio effect but, at the ends this expansion is not permitted because of the stiff end rings. The shell is, therefore, subjected to an axially symmetric radial deformation near the ends. If, however, provision is made to expand the end rings during the loading process, the deformation will be controllable and its effect can be studied.

For the current program, the rings supporting the ends of the shell were expanded by a pressure diaphragm mechanism. The test shells were copper electroformed cylinders similar to those used in previous experiments (Ref. 4). The set-up is shown in Fig. 1 in which the strain gages on the loading cylinder are used to measure the load and its distribution. The two end rings on the shell are identical and are given identical radial deformations for any specific test.

The testing procedure consists of applying an incremental axial load to the cylinder and giving the end rings a radial displacement which is some fraction of the Poisson ratio expansion of the main shell. The expansion of the end rings, δ_R, for each test is recorded at the time of buckling as well as the total load and load distribution.

The expansion of the shell, if it were free to move radially is

$$\delta_S = \nu R \frac{\sigma_{axial}}{E} = \frac{\nu P}{2\pi t E} = \frac{P}{P_{C\ell}} \frac{\nu t}{\sqrt{3(1-\nu^2)}} \qquad (1)$$

where

$$P_{C\ell} = 2\pi R t \sigma_{C\ell} = 2\pi E t^2 / \sqrt{3(1-\nu^2)} \qquad (2)$$

Table 1 and Fig. 2 show the results of 17 buckling tests for varying values of δ_R / δ_S. At $\delta_R / \delta_S = 0$, the buckling load is approximately $0.65 P_{C\ell}$ and, as would be expected, this load increases as the ratio δ_R / δ_S increases. However, it reaches a maximum at $\delta_R / \delta_S = 0.65$ and then decreases rather than going up to the expected value of $P/P_{C\ell} = 1.0$ at $\delta_R / \delta_S = 1.0$. Although this seemed to be an unexplainable anomaly at first, the reason is apparent after looking in detail at the loading apparatus.

Since, the radial expansion load is applied to the end ring only, the loading cylinder does not expand except at the point where it is attached to the end ring. This causes a very slight rotation of the end ring which, in Fig. 1 has not been considered. The objective of the program was then altered to look into the details of the slope of the cylinder in the boundary region rather than the displacement.

By using a long optical lever with a mirror attached to the end ring, the rotation of the end ring (and of the shell at the end) was measured as a function of the axial load on the shell and the radial displacement of the end ring. Once this is known, we have the radial displacement δ_R and the slope α_o of an axially loaded cylinder from which the displacements

and slopes can be found for other points along the length of the specimen. Calibration showed that the radial deflection and rotation can be given by

$$\delta_R = 0.8 \times 10^{-5} p \tag{3}$$

and

$$\alpha_R = \alpha_o = 1.2 \times 10^{-5} p + 0.12 \times 10^{-5} P \tag{4}$$

where p is the pressure in the expanding device and P is the axial load on the specimen. From (3) and (4) one can calculate the value of δ_o and α_o shown in Fig. 3, giving

$$\delta_0 = \delta_S - \left[\delta_R + \delta^*\right] \tag{5}$$

where

$$\delta^* = \ell \alpha_o \tag{6}$$

and

$$\alpha_o = 1.5 \delta_R + 0.12 \times 10^{-5} P \tag{7}$$

Calculating the slope of the shell at any point x from the end along a generator one finds

$$\alpha(x) = \left[\frac{\delta_o}{\alpha_o} \frac{2\lambda}{\sqrt{1 + \frac{P}{P_{C\ell}}}} B_{\lambda x} + C_{\lambda x}\right] \alpha_o \tag{8}$$

where

$$\lambda = \sqrt{\frac{\sqrt{3(1-\nu^2)}}{Rt}} \tag{9}$$

$$B_{\lambda x} = e^{-\beta \lambda x} \sin \gamma \lambda x \tag{10}$$

$$C_{\lambda x} = e^{-\beta \lambda x} \left[\cos \gamma \lambda x - \sqrt{\frac{\beta}{\gamma}} \sin \gamma \lambda x \right] \tag{11}$$

$$\beta = \sqrt{1 - \frac{P}{P_{C\ell}}} \qquad \gamma = \sqrt{1 + \frac{P}{P_{C\ell}}} \tag{12}$$

The location of $|\alpha|_{max}$ depends upon the values of δ_o / α_o, , and P. For example, with $P/P_{C\ell} = 0.7$ and $\lambda = 9.58$ the form of the deflected shell surface is shown in Fig. 4 for four values of δ_R / δ_S.

The value of $|\alpha|_{max}$ has been calculated for each of the shells tested and is given in Table 1. A plot of $P/P_{C\ell}$ vs $|\alpha|_{max}$ is shown in Fig. 5 and shows a definite trend of decreasing $P/P_{C\ell}$ as $|\alpha|_{max}$ increases. When one considers the magnitudes of the slopes in question the scatter of the data is not excessive. Even with extreme care, it will be difficult to obtain initial end conditions in which the slopes are known to within 10^{-3} radians (0.5 in. in 20 feet). Efforts are now being made to modify the test equipment so that essentially zero slope can be held when $\delta_R = \delta_S$ to see if values of $P/P_{C\ell}$ approaching 1.0 can be found.

REFERENCES

1. Stein, Manuel: The Influence of a Prebuckling Deformations and Stresses on the Buckling of Perfect Cylinders. NASA TR R-190, February 1964.

2. Fisher, G.: Über den Einfluss der gelenkigen Lagerung auf die Stabilität dünn wandiger Kreiszylinderschalen unter Axiallast und Innerdruck. Z. Flugwiss. 1(1963) Heft 3.

3. Sobel, L. H.: Effects of Boundary Conditions on the Stability of Cylinders Subjected to Lateral and Axila Pressures. Lockheed Missile and Space Company Technical Report 6-90-63-91, September 1963.

4. Babcock, C. D. and Sechler, E. E.: The Effect of Initial Imperfections on the Buckling Stress of Cylindrical Shells. NASA TN D-2005, July 1963.

TABLE I

Shell No.	$t \times 10^3$ inches	L	$\frac{P}{P_{Cl}}$	$\frac{\delta_R}{\delta_S}$	$\lvert\alpha\rvert_{max} \times 10^3$ radians
1	4.28	7.01	0.636	1.61	4.35
2	4.41	7.98	0.656	0	3.54
3	4.76	7.97	0.767	0.90	2.19
4	5.08	7.00	0.817	0.92	2.64
5	4.73	6.92	0.683	1.19	3.24
6	3.77	8.00	0.648	1.17	2.06
7	4.16	8.06	0.612	0	3.10
8	4.06	7.97	0.753	0.79	1.64
9	3.80	8.02	0.787	1.10	2.17
10	3.88	7.94	0.790	0.43	1.81
11	4.18	8.00	0.655	0	3.37
12	3.76	7.98	0.691	0.20	2.39
13	3.84	8.00	0.700	0.37	1.71
14	4.13	7.72	0.795	0.33	2.37
15	3.76	8.02	0.765	0.58	1.20
16	3.73	8.02	0.794	0.52	1.41
17	3.89	8.00	0.703	1.41	3.38

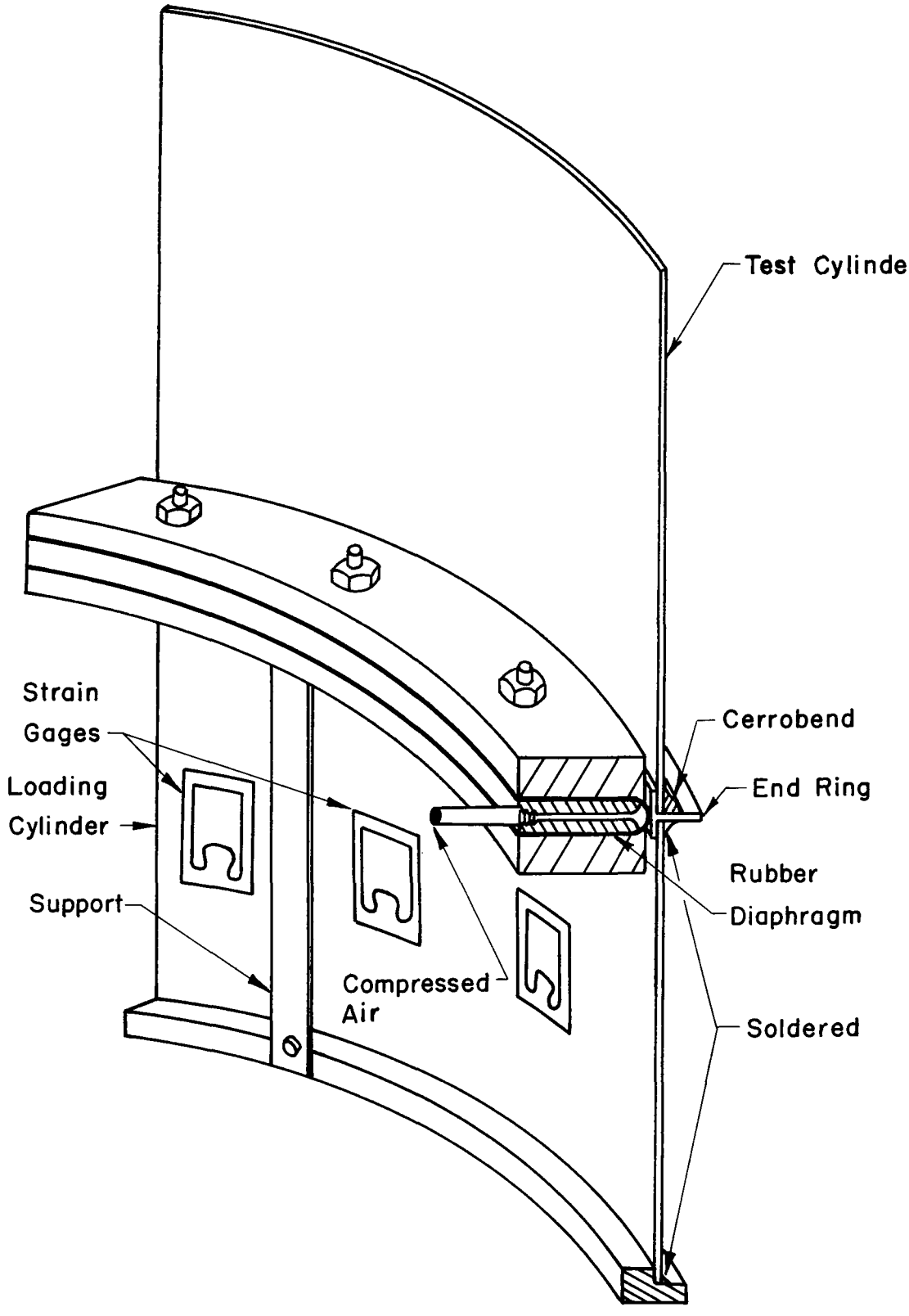
Test Cylinder
Strain
Gages
Loading
Cylinder
Support
Cerrobend
End Ring
Rubber
Diaphragm
Compressed
Air
Soldered

FIG. 1

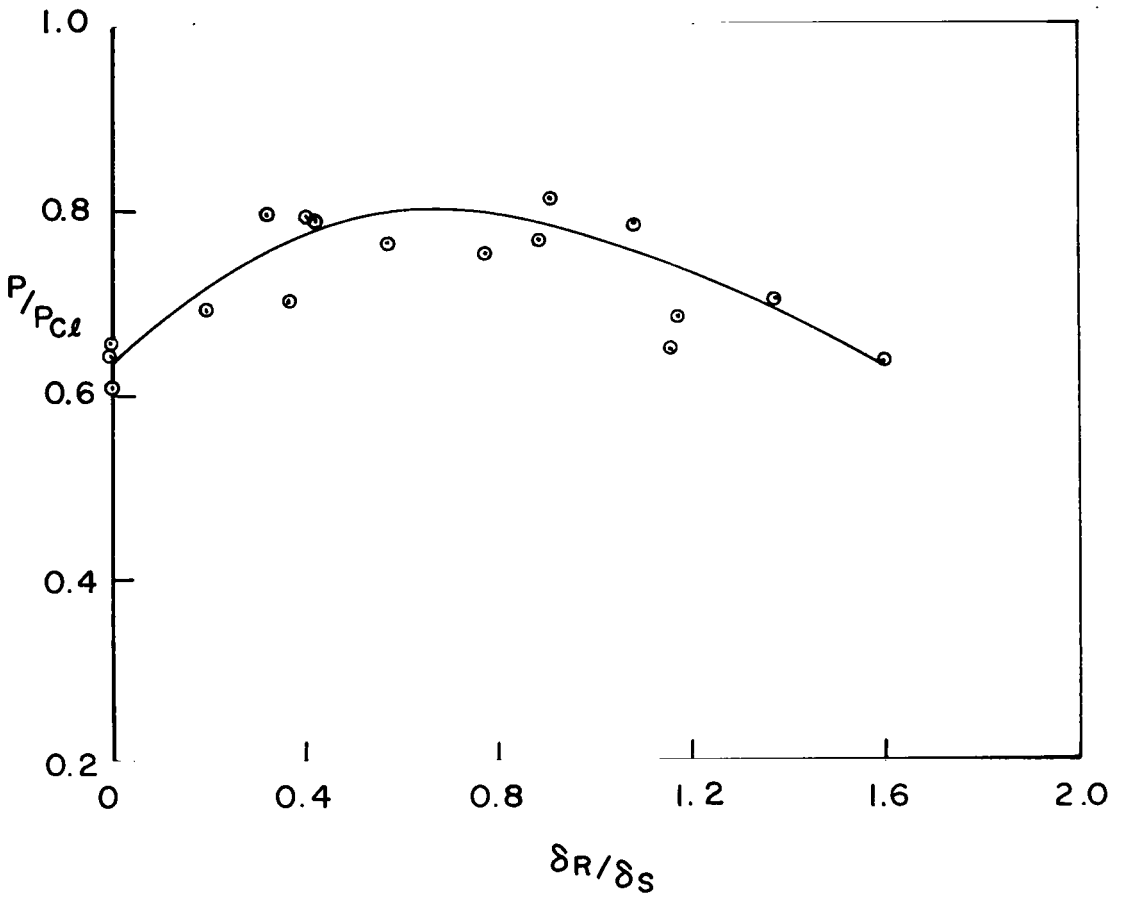

FIG. 2

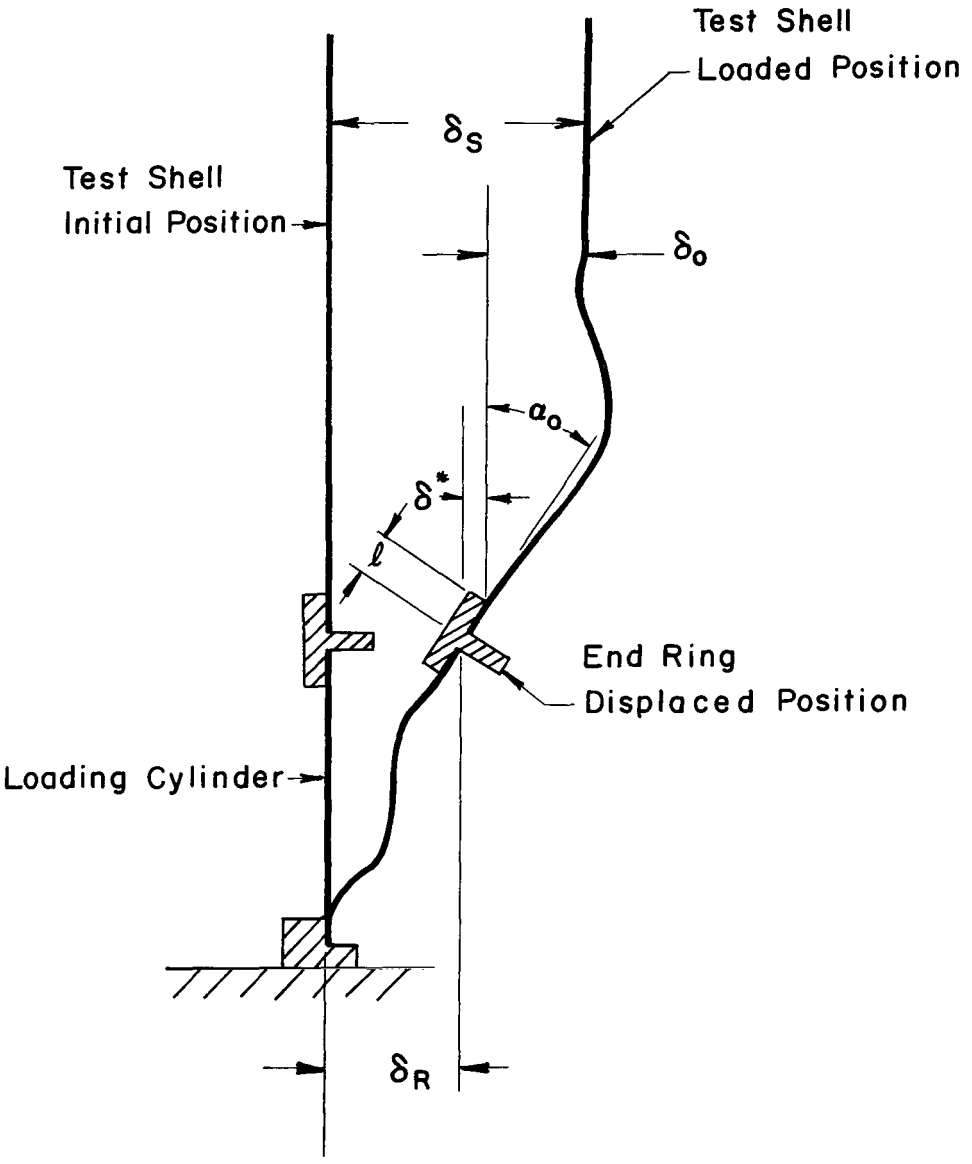
Test Shell
Loaded Position
δ_S
Test Shell
Initial Position
δ_o
α_o
δ^*
ℓ
End Ring
Displaced Position
Loading Cylinder
δ_R

FIG. 3

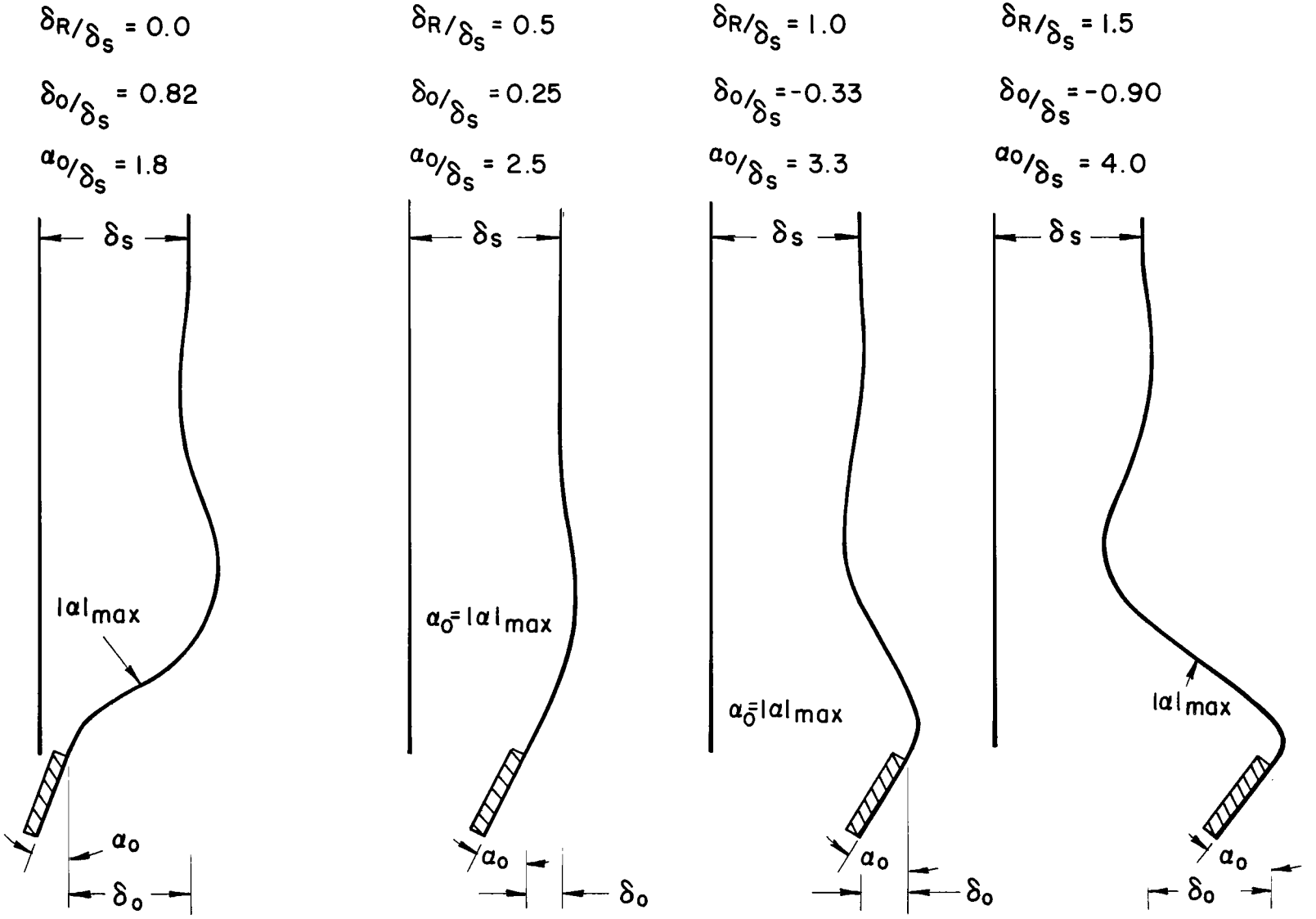
$\delta_R/\delta_s = 0.0$
$\delta_o/\delta_s = 0.82$
$\alpha_o/\delta_s = 1.8$
δ_s
$|\alpha|_{max}$
α_o
δ_o
$\delta_R/\delta_s = 0.5$
$\delta_o/\delta_s = 0.25$
$\alpha_o/\delta_s = 2.5$
δ_s
$\alpha_o = |\alpha|_{max}$
α_o
δ_o
$\delta_R/\delta_s = 1.0$
$\delta_o/\delta_s = -0.33$
$\alpha_o/\delta_s = 3.3$
δ_s
$\alpha_o = |\alpha|_{max}$
α_o
δ_o
$\delta_R/\delta_s = 1.5$
$\delta_o/\delta_s = -0.90$
$\alpha_o/\delta_s = 4.0$
δ_s
$|\alpha|_{max}$
α_o
δ_o

FIG. 4

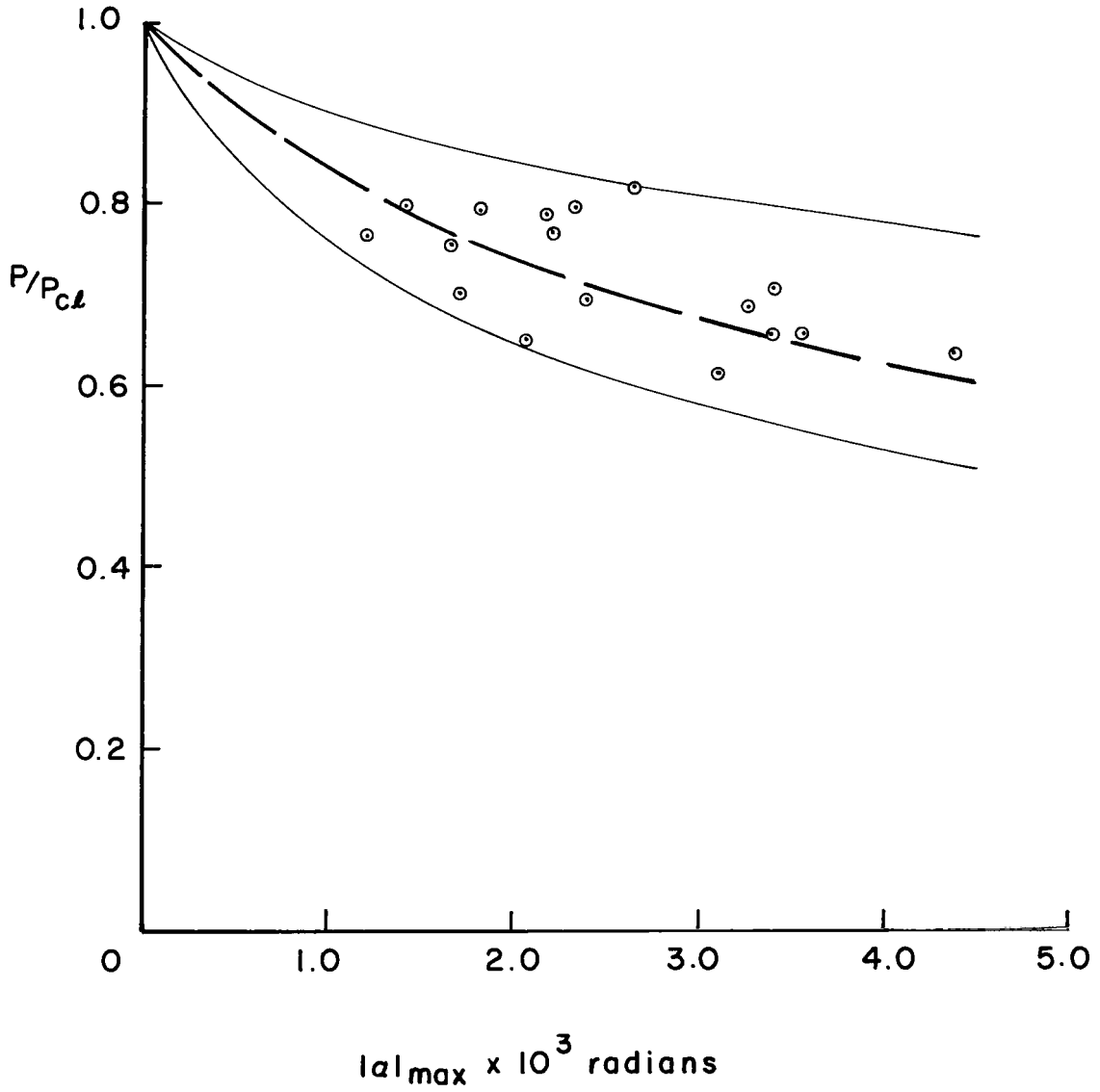

FIG. 5

NASA-Langley, 1964 D-2537

"The aeronautical and space activities of the United States shall be conducted so as to contribute . . . to the expansion of human knowledge of phenomena in the atmosphere and space. The Administration shall provide for the widest practicable and appropriate dissemination of information concerning its activities and the results thereof."

—NATIONAL AERONAUTICS AND SPACE ACT OF 1958

NASA SCIENTIFIC AND TECHNICAL PUBLICATIONS

TECHNICAL REPORTS: Scientific and technical information considered important, complete, and a lasting contribution to existing knowledge.

TECHNICAL NOTES: Information less broad in scope but nevertheless of importance as a contribution to existing knowledge.

TECHNICAL MEMORANDUMS: Information receiving limited distribution because of preliminary data, security classification, or other reasons.

CONTRACTOR REPORTS: Technical information generated in connection with a NASA contract or grant and released under NASA auspices.

TECHNICAL TRANSLATIONS: Information published in a foreign language considered to merit NASA distribution in English.

TECHNICAL REPRINTS: Information derived from NASA activities and initially published in the form of journal articles.

SPECIAL PUBLICATIONS: Information derived from or of value to NASA activities but not necessarily reporting the results of individual NASA-programmed scientific efforts. Publications include conference proceedings, monographs, data compilations, handbooks, sourcebooks, and special bibliographies.

Details on the availability of these publications may be obtained from:

SCIENTIFIC AND TECHNICAL INFORMATION DIVISION

NATIONAL AERONAUTICS AND SPACE ADMINISTRATION

Washington, D.C. 20546